

Dynamic modelling and simulation of squirrel-cage asynchronous machine with non-linear effects

Ogbonnaya I. Okoro

Department of Electrical Engineering

Faculty of Engineering

University of Nigeria, Nsukka

Enugu State, Nigeria.

Bernd Weidemann

Department of Electrical Machines

Faculty of Electrical Engineering

University of Kassel

Bernd R. Oswald

Department of Electrical Power and High Voltage Engineering

University of Hannover

ABSTRACT

The paper presents the dynamic modelling and computer simulation of a squirrel-cage induction machine with non-linear effects. The computer simulation for the transient operation is obtained from the non-linear differential system of equations which describe the induction machine in the rotor reference frame and with currents as state variables. It is shown that by using the characteristic data available from d.c. measurement, no-load, Blocked rotor and retardation tests of the machine as well as the results obtained from the optimisation of the T-model rotor circuit, accurate simulation of the machine under dynamic condition is possible. The simulated time function of the transient current, mechanical speed and shaft torque characteristics of the machine are compared with the experimental results.

KEYWORDS

Dynamic modelling, no-Load, Blocked Rotor, Skin-effect, Induction machine.

INTRODUCTION

The need for a simple, accurate and faster method

of simulating the transient performances of induction machine becomes imperative due to wide industrial applications of the machine. In the past, Analog computers have been used to study the system dynamics of induction machines (JORDAN, 1965; KRAUSE AND THOMAS, 1965). This method is, however well suited for D.C. machines since Analog computers are well adapted to handling direct voltages. A problem therefore arises when Analog computers are used in the simulation of the A.C. induction machine in dynamic systems. In (JORDAN, 1967), a software package was developed using the FORTRAN programming language and the predictor-corrector numerical technique, for the dynamic simulation of induction motor drives. Chattopadhyay (1976) uses the numerical integration technique of Runge-Kutta-Merson to simulate an Adjustable-speed induction motor drive. Both of these techniques require the development of numerical integration and inversion routines for the solution of the resultant non-linear differential equations that describe the dynamic behaviour of the machine. It will be shown in this paper that the development of such user-written program for the purpose of simulating the dynamic behaviour of A.C. induction machine is

not necessary and that a commercial software package such as MATLAB© (1991), licensed by Mathworks, presents a better alternative. By incorporating FORTRAN or C compilers, the problem of execution speed is alleviated. In MATLAB©, the integration algorithms and inversion function are efficient and accurate, thereby saving the time and energy that could have been used in writing same. This paper, therefore uses MATLAB© to develop computer program that can simulate and solve the non-linear differential equations which describe the dynamic behaviour of a squirrel-cage induction machine with saturation and skin effects. Simulation results that show the free-acceleration of the machine in rotor reference frame as well as the experimental results are presented and discussed.

INDUCTION MACHINE MODEL WITH SKIN-EFFECT

In order to accurately represent the skin-effect phenomenon in a squirrel-cage induction machine, two distinct methods have been proposed. The quasi-static method in which the steady state values of resistance and inductance are first calculated for each speed within the operating range represents the first (Haun, 1991; Humpage et al., 1969). The second method represents the eddy-currents by additional circuit equations. The equations may be in the form of lumped-parameter networks which are effectively a crude finite difference approximation to the field equations describing the eddy-current distribution (Babb and Williams, 1951). The first method produces unacceptable results at high frequencies. In this paper, therefore, the lumped-parameter networks model is applied. In order to account for changes of the rotor inductance and resistance with changes in frequency, the rotor bar is divided into sections as shown in Fig. 1.

To model the rotor bar, a T-configuration network is used according to the method proposed by Babb and Williams (1951). From Fig. 1, the rotor bar resistance and inductance for each section is,

$$R_{sec} = \frac{L_s}{\chi_{cu} h_{sec} b_{Nut}} \quad (1)$$

$$L_{sec} = \frac{\mu_o L_s h_{sec}}{b_{Nut}} \quad (2)$$

It is important to note that Eq. (1) and Eq. (2) are modified to take account of all the bars and subsequently referred to the stator to give "Rr" and "Lr" as shown in the equivalent T-circuit of the induction motor, Fig. 1b and Fig. 1c.

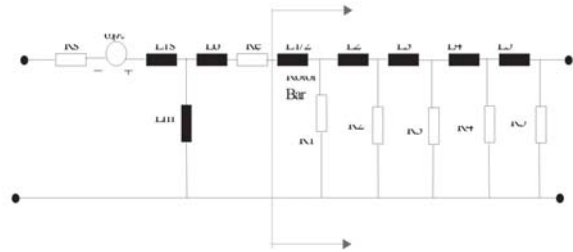


Figure 1a- Equivalent T-Circuit; Configuration for 5-section rotor bar.

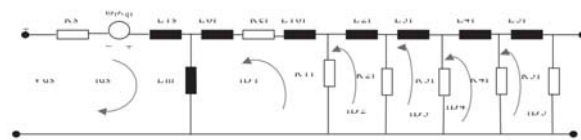


Figure 1b Equivalent circuit for d-axis with rotor values referred to the stator

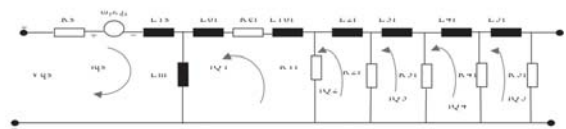


Figure 1c -Equivalent circuit for q-axis with rotor values referred to the stator

The machine d-q model equations are derived for each loop in Fig. 1 by taken the Kirchhoff's voltage expressions (Guiliemin, 1953). By using the reference frame fixed to the rotor, the voltage equations for each of the loops become:

[A] Stator Equations—(Figure 1b & Figure 1c)

Loop1

$$V_{ds} = R_s i_{ds} + L_s \frac{di_{ds}}{dt} - L_s \omega_r i_{qs} - L_m \omega_r i_{Q1} + L_m \frac{di_{D1}}{dt} \quad (3)$$

$$V_{qs} = R_s i_{qs} + L_s \frac{di_{qs}}{dt} + L_s \omega_r i_{ds} + L_m \frac{di_{Q1}}{dt} + L_m \omega_r i_{D1} \quad (4)$$

Where,
 $L_s = L_{ls} + L_m$

[B] Rotor Equations—(Figure 1b & Figure 1c)

Loop2

$$V_{D1} = 0 = (R_{er} + R_{lr})D1 - R_{lr}i_{D2} + L_{lr} \frac{di_{D1}}{dt} + L_m \frac{di_{ds}}{dt} + L_m \frac{di_{D1}}{dt} \quad (5)$$

$$V_{Q1} = 0 = (R_{er} + R_{lr})Q1 - R_{lr}i_{Q2} + L_{lr} \frac{di_{Q1}}{dt} + L_m \frac{di_{qs}}{dt} + L_m \frac{di_{Q1}}{dt} \quad (6)$$

Loop3

$$VD2 = 0 = R1riD2 - R1riD1 + R2riD2 - R2riD3 + L2r \frac{diD2}{dt} \quad (7)$$

$$VQ2 = 0 = R1riQ2 - R1riQ1 + R2riQ2 - R2riQ3 + L2r \frac{diQ2}{dt} \quad (8)$$

Loop4

$$VD3 = 0 = R2riD3 + R3riD3 - R3riD4 - R2riD2 + L3r \frac{diD3}{dt} \quad (9)$$

$$VQ3 = 0 = R2riQ3 + R3riQ3 - R3riQ4 - R2riQ2 + L3r \frac{diQ3}{dt} \quad (10)$$

Loop5

$$VD4 = 0 = R4riD4 + R3riD4 - R3riD3 - R4riD5 + L4r \frac{diD4}{dt} \quad (11)$$

$$VQ4 = 0 = R4riQ4 + R3riQ4 - R3riQ3 - R4riQ5 + L4r \frac{diQ4}{dt} \quad (12)$$

Loop6

$$VD5 = 0 = R5riD5 + R4riD5 - R4riD4 + L5r \frac{diD5}{dt} \quad (13)$$

$$VQ5 = 0 = R5riQ5 + R4riQ5 - R4riQ4 + L5r \frac{diQ5}{dt} \quad (14)$$

MODEL DEVELOPMENT WITH SATURATION EFFECT

The values of the inductances used in the development of the dynamic equations for the classical and skin-effect induction machine models were assumed to be constant. By so doing, the models fail to take into consideration the saturation effects of the magnetizing field. It has been proved beyond doubts by several authors (Melkebeek, 1983; Mello; Walsh, 1961; He, Lipo, 1984) that the stability and dynamic conditions of induction machine are highly affected by saturation. Several methods have been developed in modelling saturation effect in induction machines (Lipo; Consoli, 1984); (Keyhani; Tsai, 1989); (Boldea; Nasar, 1988); (Levi, 1995); (Slemon, 1989)-each differing in area of applications and of course, in the part of the machine inductances that are assumed to saturate. In (Lipo; Consoli, 1984; ; Keyhani Tsai, 1989), induction motor with saturable leakage reactances is modelled and simulated with the help of analog computer and IGSPIICE respectively. In He (1984) and Levi (1995) the effect of considering the main flux saturation is investigated. A saturation model for leakage inductances presents a difficult task in terms of analysis and computer time (Lipo; Consoli, 1984; ; Keyhani, Tsai, 1989; Slemon, 1989). It has been shown however, that the main magnetizing field contributes significantly to the disparity between induction machines computer simulation results and experiment (He and Lipo, 1984). Therefore, to a very high level of

accuracy the effects of saturation in induction machines can be included by variation of the main flux inductance while assuming the leakage inductances to be constant. However, where the stator and rotor currents are expected to be very high values, inclusion of the leakage inductance saturation becomes imperative (Lipo; Consoli, 1984; Keyhani; Tsai, 1989). In this paper, saturation due to the influence of the main flux inductance is considered. The application of this method requires that the no-load saturation curve of the machine be known. The saturation curve of the induction motor determined by taking the motor no-load current measurements with balanced 3-phase, 50Hz voltages applied to the stator windings without mechanical load on the motor is shown in Fig. 2. The voltage increments start below rated voltage on the linear portion of the curve and normally continue to somewhat above rated voltage well beyond the knee of the curve.

It is important to add that measurements above rated voltage should be taken as quickly as possible to avoid over heating of the stator windings and consequent breakdown of the machine. Because the loss component of no-load current is very low compared to the magnetizing component, the measured no-load current values may be assumed to be all flux-producing currents without loss in accuracy.

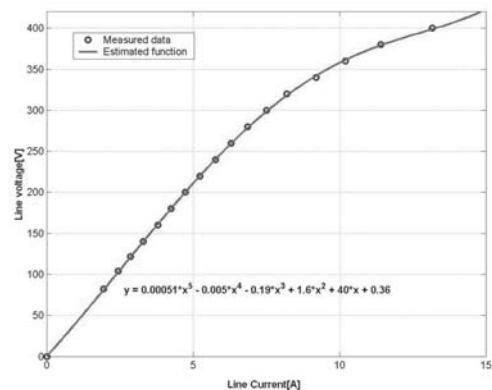


Figure .2 - no-load Saturation curve.

Due to very low slip at no-load, the secondary branch impedances become very high referred to the stator. This practically eliminates the participation of the rotor circuit leaving only the stator leakage (Lls) and the magnetizing branch (Lm) to contribute to the no-load saturation curve shown in Fig. 2. Since the stator leakage inductance, Lls is assumed constant, then

the magnetizing inductance can be extracted from Fig. 2.

In order to find an analytical expression for the saturation characteristic curve, a curve-fitting method which employs the algorithm of Marquardt (1963) is employed. Figure 3 shows the approximated curve with the estimated function as:

$$L_m = 0.064i_m^4 - 0.94i_m^3 + 2.4i_m^2 - 1.4i_m + 230[mH] \quad (15)$$

By storing the analytical expression in the computer, the value of the magnetizing inductance in the Skin-effect model can be updated at each integration step.

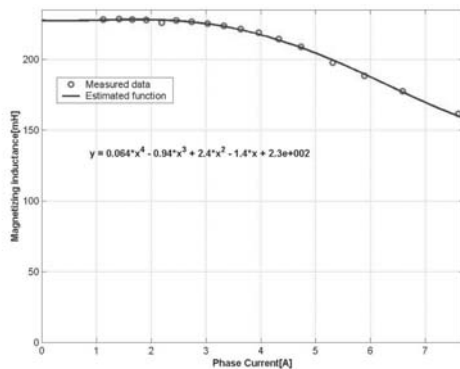


Figure 3- Saturation Curve and Polynomial approximation.

MECHANICAL MODEL

The mechanical model of the machine including the coupling system but with damping factor (d_w) neglected can be expressed as in (Okoro, 2002):

$$\begin{bmatrix} \dot{\omega}_m \\ \dot{\omega}_{mL} \\ \dot{M}_w \end{bmatrix} = \begin{bmatrix} 0 & 0 & -\frac{1}{J_{m1}} \\ 0 & 0 & \frac{1}{J_L} \\ c_w & -c_w & 0 \end{bmatrix} \begin{bmatrix} \omega_m \\ \omega_{mL} \\ M_w \end{bmatrix} + \begin{bmatrix} \frac{T_e}{J_{m1}} \\ -\frac{T_L}{J_L} \\ 0 \end{bmatrix} \quad (16)$$

The Electromagnetic torque, T_e is given as:

$$T_e = \frac{3}{2} PL_m (i_{qs} i_{dr} - i_{ds} i_{qr}) \quad (17)$$

EXPERIMENTAL VERIFICATION

The test machine is a **KATT VDE 0530**, Class F insulation, surfaced-cooled squirrel-cage induction motor. The rated power, speed, and current are 7.5KW, 1400rpm and 19.2A respectively. The test machine is a four-pole motor with 50Hz rated frequency and 340V rated voltage. Several experiments were carried out on the test machine. The no-load test was carried out at rated frequency and with balanced polyphase voltages applied to the stator terminals. Readings for

current, voltage, electrical power and speed were taken after the motor has been running for a considerable long period of time necessary for the bearings to be properly lubricated. Locked-rotor test and test with the injection of D.C. current in the stator windings were made at standstill. The retardation test was carried out at no-load with and without additional standard mass.

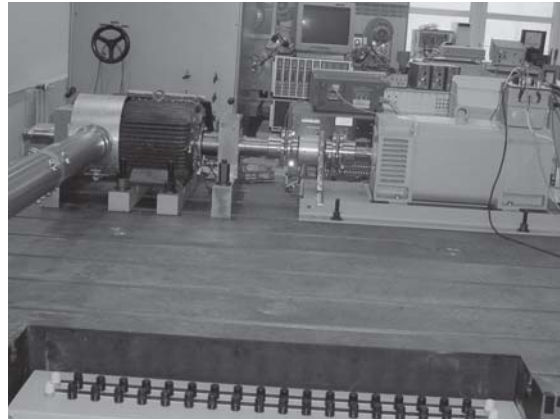


Figure 4- Test machine experimental set-up during rated load operation.

Test machine(A), Coupling system(B), Digital-Real-Time Oscilloscope(C), Load D.C. machine(D), Mechanical speed leads(E), Computer(F).

The load test was carried out with constant load and frequency at a sinusoidal stator windings voltage. The test machine is star-delta connected, operated as motor and was loaded by 7.6KW D.C. machine as shown in Fig.4. Measurements of the test machine's transient stator currents, stator voltages, shaft torque and speed were made during run-up of the machine.

The mechanical speed leads (E) as shown in Fig.4 were taken through the speed terminals of the tachogenerator and connected to one of the channels of Digital Real-Time Oscilloscope, DRTO (C). The tachogenerator analog output is 20V per 1000rpm. The shaft torque was measured by using the 22/100 DATAFLEX torque measuring instrument connected together with the coupling system (B). The torque measuring instrument has as its output, voltage which was read through the DRTO. Three FLUKE current probes but with the same setting were used to measure the transient stator phase currents at run-up operation. All the run-up operation measurements were recorded in real time via a four-channel TS 200-series DRTO with RS232 output terminal. The RS232 output terminal enables the output from the DRTO to be monitored through a computer (F).

INDUCTION MACHINE MODEL SIMULATION

In order to simulate the induction motor transient model, the loop equations, together with equation (15), equation (16) and equation(17) are solved by developing MATLAB© (1991) m-files which incorporate an in-built numerical algorithm, ODE45-a program that uses Runge-Kutta numerical method. The simulations have been carried out using the motor data obtained from the open circuit, short circuit, D.C. measurement and retardation tests of the motor under study (Appendix A) and the estimated rotor parameters(Appendix B). An optimisation algorithm is incorporated into the m-files from which the estimated rotor parameters are obtained. The optimised model as shown in Fig. 5 closely matches with the actual rotor bar characteristics of the machine. At approximately 4KHz frequency, the error in the developed model is about 6%. Figure 6 shows the predicted transient characteristics of the test machine during free acceleration with skin and saturation effects. Figure 7 shows the measured run-up transient characteristics of the test machine. Comparison between Fig. 6 and Fig. 7 shows that the predicted results closely match the measured results. However, the errors that exist in the predicted results may be as a result of the stator and rotor resistances which were assumed to be constant throughout the transient operation. This may not be necessarily so as the resistances are dependent on temperature—which in itself increases as the machine is in operation. Again, it is envisaged that consideration of the leakage inductances as being saturated may improve the simulated results. The mechanical model of the machine has been developed neglecting the damping factor and the friction in the bearing system. This definitely will diminish the accuracy of the predicted shaft torque.

CONCLUSION

The paper has shown that the MATLAB© software package is highly suitable for the dynamic simulation of induction machine model with saturation and skin effects. By optimising the rectangular-shaped rotor bar, a good correction between the model impedance and the actual rotor bar impedance could be achieved. The simulated machine model with saturation and skin effects included gives comparatively good result and can therefore be conveniently used to predict the actual machine performances in dynamic states.

However, by making the stator and rotor resistances to be temperature dependent and by incorporating the damping factor and frictional loss coefficients in the mechanical systems equations, more better results could be achieved.

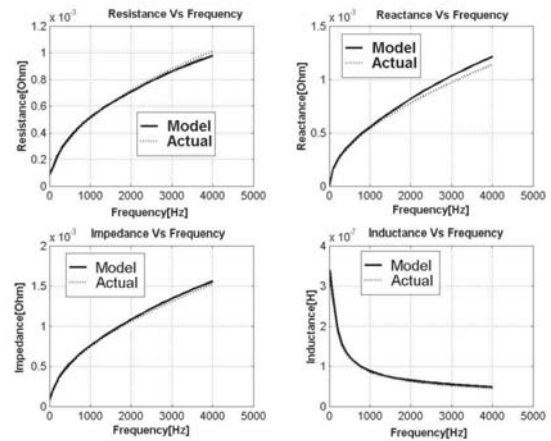


Figure 5 - Bar-Model plots for bar sections(100) and model sections(5).

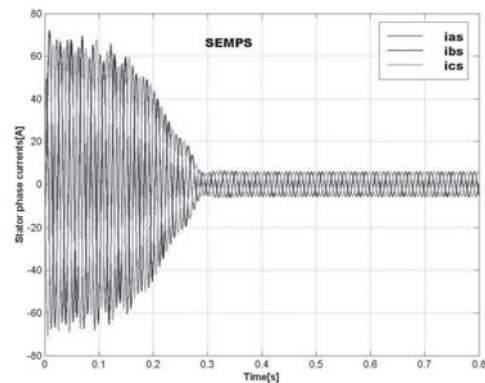


Figure 6a - Skin-effect model plus saturation(SEMPS) simulation: Stator phase currents at run-up.

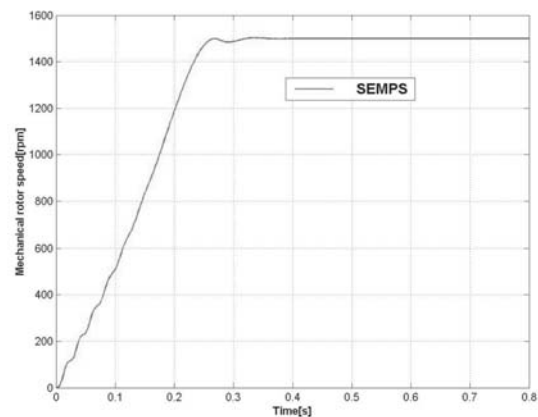


Figure 6b - Skin-effect model plus saturation(SEMPS) simulation: Mechanical rotor speed at run-up.

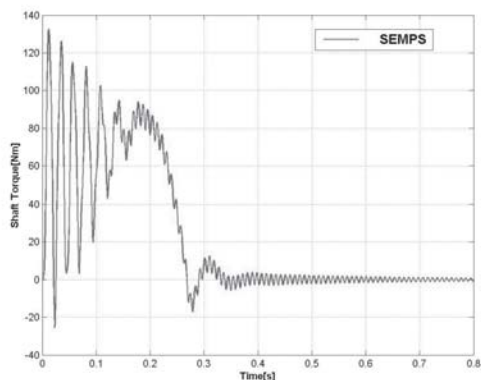


Figure 6c - Skin-effect model plus saturation(SEMPs) simulation: Shaft torque at run-up.

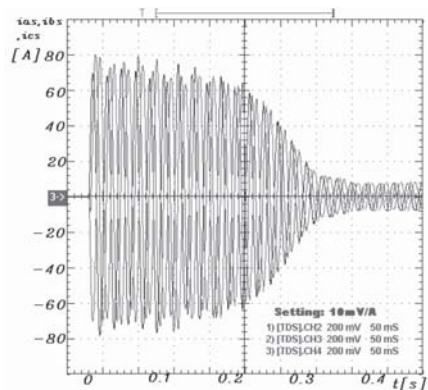


Figure 7a - Measurement: Stator phase currents at run-up(Delta connected, $V_{rms} = 340V$).

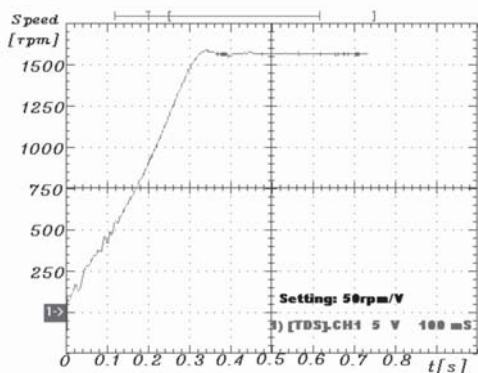


Figure 7b - Measurement: Mechanical rotor speed at run-up(Delta connected, $V_{rms}=340V$).

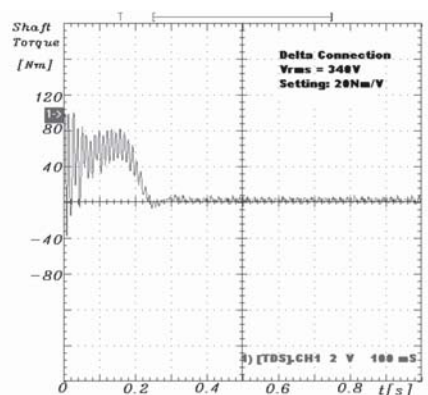


Figure 7c - Measurement: Shaft torque at run-up(Delta connected, $V_{rms} = 340V$, Setting:20Nm/V).

ACKNOWLEDGEMENTS

The Authors wish to express their thanks to **DAAD** for her financial support.

REFERENCES

- BABB, D.S. WILLIAMS, J.E. Network analysis of A.C. machine conductors. AIEE Transactions, vol. 70, p.2001-2005, 1951.
- BOLDEA, I. AND NASAR, S. A. A general Equivalent circuit(GEC) of electric machines including cross-coupling saturation and frequency effects. IEEE Transactions on Energy Conversion, v.3, p.689-695. 1988.
- CHAHOPADHYAY, A.K. Digital computer simulation of an Adjustable-speed induction motor drive with a cycloconverter type thyristor-commutator in the rotor. IEEE transaction on industrial Electronics and control instrumentation, p.86-92, 1976.
- MELLO, F. P. AND WALSH, G.W. Reclosing Transients in

induction motors with Terminal Capacitors. AIEE Transactions, Willey, p. 1206-1213, 1961.

GUILIEMIN, E.A. Introductory Circuit Theory. New-York: Willey, 1953.

HAUN, A. Vergleich von Steuerverfahren für Spannungseinprägende Umrichter Zur Speisung von Käfigläufermotoren. PhD Thesis (_____-) University of Darmstadt.

HE,Y.; LIPO, T.A. Computer Simulation of an induction machine with spatially dependent saturation. IEEE Transactions on Power Apparatus and systems, v. 103, n.4, p.707-714, 1994.

Humpage, W.D. et al. Dynamic response analysis of interconnected synchronous-asynchronous machine groups. Pro. IEE, v. 166, n. 2, p. 2015-2027, 1969.

JORDAN, H.E. Analysis of induction machines in dynamic systems. IEEE Transactions on Power Apparatus and systems, v. 84, n. 11, p.1050-1088, 1965.

_____. Digital computer Analysis of of induction machines in dynamic systems. IEEE Transactions on Power Apparatus and systems, vol. 86, n. 6, p. 722-728, 1967.

KEYHANI, A.; TSAI, H. IGSPICE simulation of induction machines with saturable inductances. IEEE Transactions on Energyconversion, v. 4, n. 1, p.118-125.

KRAUSE, P.C.; THOMAS, C.H. Simulation of symmetrical induction machinery. Transaction IEEE, v. 84, n.11, p.1038-1053, 1965.

LEVI, E. A unified approach to main flux saturation modelling in D-Q axis models of induction machines. IEEE Transactions on Energy conversion, v.10, n.3, p. 455-460, 1995.

LIPO, T.A. AND CONSOLI, A. Modeling and simulation of induction motors with saturable leakage reactances. IEEE Transactions on industry Applications, v. 20, n.1, p.180-189, 1984.

MARQUARDT, D.W. An Algorithm for least-square estimation of non-linear parameters. J. Soc. Ind. Appl. Math, v. 11, n.2, p.431-441, 1963.

MATLAB User's Guide, 1991. The Mathworks, Inc, Cochituate Place, 24 Prime Parkway, Natick.

MELKEBEEK, J.A.A. Magnetizing –field saturation and dynamic behaviour of induction machines. Part 1: Improved calculation method for induction-machine dynamics. IEE Proc. v. 130, n.1, p.1-9, 1983.

OKORO, O.I. Dynamic and thermal modelling of induction machine with non-linear effects. Kassel University, 2002.

SLEMON, G.R. Modelling of induction machines for electric drives. IEEE Transactions on Industry Applications, v.25, n.6, p.1126-1131, 1989.

Appendix A. Machine data

Output Power	7.5KW
Rated voltage	340V
Winding connection	Delta
Number of Poles	4
Rated speed	1400rpm
Rated frequency	50Hz
Stator resistance	2.52195ohm
Stator leakage reactance	1.95145ohm
Rotor resistance	0.976292ohm
Rotor leakage reactance	2.99451ohm
Magnetizing reactance	55.3431ohm
Mechanical shaft torque	51.2636N.m
Estimated rotor inertia moment	0.117393Kgm ²
Rated current	19.2A
Moment of inertia of the D.C. motor	0.10958Kgm ²
Shaft stiffness constant	14320Nm/rad

Appendix B. Estimated Rotor Circuit Parameter

Resistance	[mΩ]	Inductance	[μH]
R ₁	1.338	L ₁	6.1150e-2
R ₂	0.656	L ₂	9.2940e-2
R ₃	0.321	L ₃	0.1896
R ₄	0.179	L ₄	0.3562
R ₅	1.338	L ₅	0.2596